

# Characterization of $\text{In}_{1-x}\text{Cd}_x\text{S}$ , $\text{In}_2\text{S}_3$ and CdS thin films grown by SILAR method

Mutlu Kundakçı<sup>1</sup>

Received: 16 September 2016 / Accepted: 19 December 2016 / Published online: 27 January 2017  
© Springer Science+Business Media New York 2017

**Abstract** Successive Ionic Layer Adsorption and Reaction (SILAR) technique was used to deposit  $\text{In}_{1-x}\text{Cd}_x\text{S}$ ,  $\text{In}_2\text{S}_3$  and CdS thin films on glass substrate at room temperature. The crystal structure and crystal size of the thin films were characterized by X-ray diffraction (XRD) method. Scanning Electron Microscopy (SEM) was used to determine morphology and composition of the films. Optical and electrical properties of these films have been investigated as a function of temperature. The photoluminescence measurements were carried out at room temperature and absorption measurements were carried out in the temperature range 10–320 K with a step of 10 K. The band gap energies for CdS,  $\text{In}_{0.8}\text{Cd}_{0.2}\text{S}$ ,  $\text{In}_{0.6}\text{Cd}_{0.4}\text{S}$ ,  $\text{In}_{0.4}\text{Cd}_{0.6}\text{S}$ ,  $\text{In}_{0.2}\text{Cd}_{0.8}\text{S}$  and  $\text{In}_2\text{S}_3$  thin films were found as 2.22 eV, 2.56 eV, 2.52 eV, 2.46 eV, 2.38 eV, and 2.72 eV, respectively. The refractive indices ( $n$ ), optical static and high frequency dielectric constants ( $\epsilon_0$ ,  $\epsilon_\infty$ ) values have been calculated by using the energy bandgap values. The electrical resistivity of CdS,  $\text{Cd}_{0.5}\text{In}_{0.5}\text{S}$  and  $\text{In}_2\text{S}_3$  thin films have been determined using a ‘dc’ two probe method, in the temperature range of 300–450 K. The electrical resistivity values have been calculated at 300 K.

## 1 Introduction

Semiconductor materials, which can be grown efficiently as thin films with low cost, are used extensively for a variety of applications, including architectural windows, solar

cells, heat reflectors, light transparent electrodes, and thin film photovoltaic and many other optoelectronic devices. Cadmium sulfide thin films have received considerable attention due to their applications in thin film solar cells, electrochemical cells and semiconductor metal Schottky barrier cells. CdS does not play a direct role in photovoltaic conversion of solar radiation; however, it is adequate as an optical window and preferred over other materials of wide band gap due to their compact crystallographic cell and electronic affinity with  $\text{CuInSe}_2$ , InP, CdTe and other p-type semiconductors used as absorbers. The properties of CdS thin films obtained by several techniques, such as close spaced vapor transport [1], chemical bath deposition [2, 3], femtosecond pulsed laser deposition [4], and SILAR [5, 6] have generated a great amount of information about its physical properties. Optical band gap of CdS was found as 2.42 eV by Tong et al. [4]. The band gap energy varies as found from 2.1 to 2.4 eV [3]. The most common phase of CdS bulk crystals is the hexagonal structure [3, 4].

In recent years, there has been a significant increase in the research works on III-VI materials, because of the enhanced interest due to their enhanced applications in optoelectronics and/or photovoltaic device fabrication. Indium sulfide ( $\text{In}_2\text{S}_3$ ) is a III-VI compound, originating from II-VI semiconductor, by replacing group II metals by group III elements. Solar cells based on heterostructures using CdS as the window buffer layer have been the focus of intensive research in the last few years because they have attained very promising conversion efficiencies. Presently, efforts are there for replacing CdS by indium sulfide thin films to avoid toxic cadmium, in order to make photovoltaic technology more ecofriendly. For these reasons, it is important to investigate about other semiconductor materials with the appropriate properties to substitute the CdS buffer layer in the solar cell heterostructure. One of the

✉ Mutlu Kundakçı  
kundakci@atauni.edu.tr

<sup>1</sup> Department of Physics, Science Faculty, Atatürk University, Erzurum, Turkey

most promising semiconductor materials studied is  $\text{In}_2\text{S}_3$ . There are reports about solar cells based on  $\text{CuInS}_2/\text{In}_2\text{S}_3$  heterostructures that have achieved efficiencies as high as 9.5% [7]. It can be prepared using different chemical techniques such as chemical spray pyrolysis (CSP) [8–10], thermal evaporation technique [11, 12] electrodeposition [13], chemical bath deposition (CBD) [14] and SILAR [5, 15, 16]. The optical properties of indium sulphide ( $\text{In}_2\text{S}_3$ ) thin films depend on their synthesis process and on their composition. The energy band gap for the as-deposited  $\text{In}_2\text{S}_3$  was found to be 2.60 eV and 2.70 eV [11, 15]. The most common phase of  $\text{In}_2\text{S}_3$  thin film is the cubic structure [12].

Ternary metal chalcogenide composite thin films have attracted considerable attention because of their interesting size dependent properties and wide range of applications in optical fibers, light emitting diodes, sensors, solar cells etc. The interesting characteristics and related applications were dominated by several factors, such as surface morphology, grain size, crystallinity, band gap and resistivity etc. In the literature, the reports are available on the formation of separate phases of chemically deposited ternary thin films such as,  $\text{CdZnS}$ ,  $\text{CdInS}$  and  $\text{CdZnSe}$  etc.  $\text{In}_{1-x}\text{Cd}_x\text{S}$  ( $\text{InCdS}$ ) ternary compounds can form a continuous series of solid solution allowing systematic variation in the band gap of  $\text{InCdS}$  from 2.20 eV for  $\text{CdS}$  to 2.72 eV for  $\text{In}_2\text{S}_3$  by adjusting the composition.  $\text{In}_2\text{S}_3$  and  $\text{In}_{1-x}\text{Cd}_x\text{S}$  and  $\text{CdS}$  thin films were grown on glass substrates by using Successive Ionic Layer Adsorption and Reaction (SILAR) technique at room temperature. The band gap energies of the films were determined by optical absorption measurements as a function of temperature. It has been seen that, the band gap energies of are decreasing with in increasing temperature [17].  $\text{In}_{1-x}\text{Cd}_x\text{S}$  thin films are new materials in literature. Thus, it is important to know properties of these materials. In this paper, we have studied physical properties of  $\text{In}_{1-x}\text{Cd}_x\text{S}$ ,  $\text{In}_2\text{S}_3$  and  $\text{CdS}$  thin films which were grown by SILAR method. Also, refractive index ( $n$ ), optical static and high frequency dielectric constants of semiconductors are important for several electron-device properties. Hence the possible application (photonic crystals, wave guides, detectors) of semiconductors in optical and optoelectronic devices depends on knowing these characteristic values [18].

## 2 Experimental details

### 2.1 Sample preparation

Semiconductor thin films are fabricated by several methods both in gas and liquid phases. In comparison to gas phase methods, liquid phase methods have an advantage of providing thin films of large area at low cost but have a

disadvantage in terms of difficulty in the control of a precise film structure. One of the liquid phase methods for deposition of thin films is SILAR method. The SILAR method was developed by Nicolau for the deposition of zinc and cadmium chalcogenides thin films some 15 years ago [19].

In this method, thin films are fabricated by alternate dipping into two solutions of each precursor ion for compound semiconductors. Therefore, the control of the film thickness becomes feasible by changing the number of the dipping cycles. Furthermore, atomically controlled multilayer thin films or super lattices can possibly be fabricated by changing precursor solutions. Since the SILAR method depends only on immersing the substrate into the solutions, the deposition of films with a large area can be achieved at low cost.

$\text{In}_2\text{S}_3$ ,  $\text{CdS}$  and  $\text{In}_{1-x}\text{Cd}_x\text{S}$  ( $x=0.2, 0.4, 0.6, 0.8$ ) thin films have been deposited on a glass substrate using SILAR method at room temperature. This is one of the first studies which deposition of the  $\text{In}_{1-x}\text{Cd}_x\text{S}$  thin films by using the SILAR method. The adsorption, reaction and rinsing times were chosen experimentally so that deposition occurred layer wise and resulted in homogeneous thin film structure. The substrate materials cleaned using an ultrasonic bath with acetone and water–ethanol (50:50) solution and dried. For the deposition of  $\text{In}_2\text{S}_3$  thin film, 0.1 M  $\text{InCl}_3$  solution ( $\text{pH}\sim 5.5$ ) is used as cationic precursor and 0.05 M  $\text{Na}_2\text{S}$  solution ( $\text{pH}\sim 11.5$ ) as anionic precursor. The well-cleaned glass substrates were immersed in the cationic precursor solution ( $\text{InCl}_3$ ) for a particular timing resulting in the adsorption of Indium ions on the surface of glass substrate. Then substrate was immersed doubly distilled water for another period of time to prevent homogenous precipitation. It was followed by immersion in the anionic precursor solution ( $\text{Na}_2\text{S}$ ) for a third period of timing. Sulfide ions react with the adsorbed indium ions on the glass substrate resulting in the formation of  $\text{In}_2\text{S}_3$  layer. The substrate was immersed in doubly distilled water again and this completes one SILAR cycle. For the deposition of  $\text{CdS}$  thin film, a well-cleaned glass substrate was immersed in the cationic precursor solution ( $\text{CdCl}_2$ ) for 40 s, causing cadmium ions to be adsorbed on the surface of the glass substrate. This substrate was immersed in doubly distilled water for 50 s to prevent homogenous precipitation. The substrate was then immersed in the anionic precursor solution ( $\text{Na}_2\text{S}$ ) for 40 s. Sulfide ions reacted with the adsorbed cadmium ions on the glass substrate. The substrate was then immersed in double-distilled water for 50 s. Thus, one cycle of  $\text{CdS}$  film deposition is completed. For the deposition of  $\text{In}_{1-x}\text{Cd}_x\text{S}$  thin films, the concentrations of cadmium chloride and indium chloride were optimized to deposit good quality and stoichiometric  $\text{In}_{1-x}\text{Cd}_x\text{S}$  composite thin films. The well-cleaned glass substrates were immersed in the cationic

precursor solution (CdCl<sub>2</sub> + InCl<sub>3</sub>) for a particular timing resulting in the adsorption of Indium and Cadmium ions on the surface of glass substrate. Then substrate was immersed doubly distilled water for another period of time to prevent homogenous precipitation. It is followed by immersion in the anionic precursor solution (Na<sub>2</sub>S) for a third period of timing. Sulfide ions react with the adsorbed indium and cadmium ions on the glass substrate resulting in the formation of In<sub>1-x</sub>Cd<sub>x</sub>S layer. The substrate is immersed in doubly distilled water again and this completes one SILAR cycle. By the repeating such SILAR cycles 100 times, we obtained In<sub>1-x</sub>Cd<sub>x</sub>S, In<sub>2</sub>S<sub>3</sub> and CdS thin films. Optimized preparative parameters for CdS and In<sub>2</sub>S<sub>3</sub> thin films have been given in Table 1.

**2.2 Structural and morphological analysis**

The films thicknesses were calculated within the limit of experimental errors by using optical interference method. The films thicknesses have been given in Table 2. For structural studies, Rigaku 2200D/Max, X-ray diffractometer using Cu Kα (λ=1.5405 Å) radiation in the 2θ range 20-100° was used. For studying surface morphology, scanning electron microscopy (SEM, JEOL-JSM5600) was used.

**2.3 Absorbance and photoluminescence measurements**

Optical properties of these films have been investigated as a function of temperature. The optical properties of the films have been studied via absorption measurements as a function of temperature with Perkin Elmer UV/VIS Lambda 2 S spectrometer which wavelength resolution better than ± 3 nm in the wavelength 190–1100 nm and a closed cycle He cryostat was used. Optical absorption measurements have been done in the temperature range 10-320K with 10 K steps and in every temperature, 10 min waited for temperature stabilization. The band gap energy changing investigated as a function of temperature. Measurement of PL emission at room temperature was made with Shimadzu RF-5301 PC spectrofluorimeter.

**Table 2** Thicknesses of In<sub>2</sub>S<sub>3</sub>, In<sub>1-x</sub>Cd<sub>x</sub>S and CdS Semiconductors Thin Films

Sample	Thicknesses (nm)
In <sub>2</sub> S <sub>3</sub>	330 ± 14
In <sub>0.2</sub> Cd <sub>0.8</sub> S	330 ± 13
In <sub>0.4</sub> Cd <sub>0.6</sub> S	328 ± 14
In <sub>0.6</sub> Cd <sub>0.4</sub> S	330 ± 13
In <sub>0.8</sub> Cd <sub>0.2</sub> S	320 ± 15
CdS	320 ± 15

**2.4 Electrical measurements**

The electrical resistivity of these films were measured using a two-probe method in the temperature range of 300–450 K by defining area of 0.2 cm<sup>2</sup> on film and for good ohmic contacts, silver paste used. For accurate measurement of temperature, digital temperature controller (Lake Shore) based on PT-100 sensor of accuracy ± 1 °C was used.

**3 Result and discussion**

**3.1 Structural studies**

The XRD patterns of CdS, In<sub>2</sub>S<sub>3</sub> and In<sub>1-x</sub>Cd<sub>x</sub>S thin films are shown in Fig. 1. Diffraction angles and Miller indices of the peaks are shown in the figures and have been given in Table 3. For Cadmium compositions x=0.2, 0.4, 0.6 and 0.8 the crystal line structure of the In<sub>1-x</sub>Cd<sub>x</sub>S films have been determined from X-ray diffraction analysis. As shown in Fig. 1, In<sub>1-x</sub>Cd<sub>x</sub>S composite thin films are polycrystalline, with well-defined diffraction peaks that corresponds to cubic phase of In<sub>2</sub>S<sub>3</sub> and hexagonal phase of CdS confirming formation of In<sub>1-x</sub>Cd<sub>x</sub>S. It is clearly observed that number of characteristic diffraction peaks of CdS is increasing with the increasing of cadmium molar fraction (x=0.2, 0.4, 0.6, 0.8).

For CdS the strong XRD peaks at ±26.5° correspond to diffraction angles of the (002) plane of hexagonal CdS [3–6, 20]. The found peaks (101), (200), (102), (110), (112) are reported as the characteristic peaks for CdS thin films by several workers [3, 4, 18]. The characteristic diffraction peaks

**Table 1** Optimized preparative parameters for CdS, In<sub>1-x</sub>Cd<sub>x</sub>S and In<sub>2</sub>S<sub>3</sub> thin films

Parameters	Precursors solutions					
	CdS		In <sub>1-x</sub> Cd <sub>x</sub> S		In <sub>2</sub> S <sub>3</sub>	
	CdCl <sub>2</sub>	Na <sub>2</sub> S	CdCl <sub>2</sub> + InCl <sub>3</sub>	Na <sub>2</sub> S	InCl <sub>3</sub>	Na <sub>2</sub> S
Concentration (M)	0.1	0.05	0.1	0.05	0.1	0.05
pH	~5.9	~11.5	~5.7	~11.5	~5.5	~11.5
Immersion time (seconds)	40	40	40	40	40	40
Number of SILAR cycles	100	100	100	100	100	100

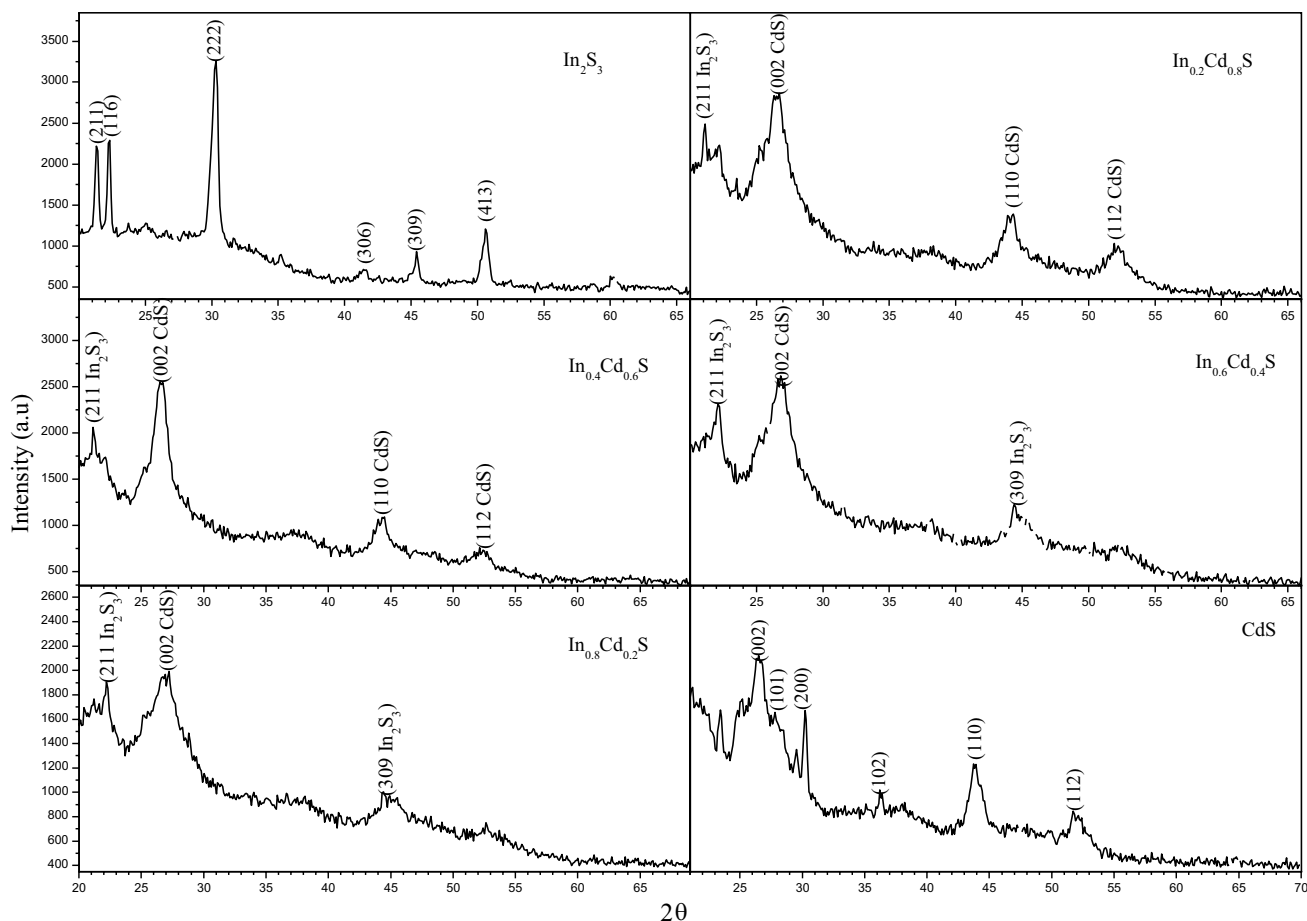


**Fig. 1** The XRD Pattern of  $\text{In}_2\text{S}_3$ , CdS and  $\text{In}_{1-x}\text{Cd}_x\text{S}$  thin films

which indicate cubic structure of  $\text{In}_2\text{S}_3$  are (211), (116), (222), (306), (309), (413) planes [10–13, 15, 21].

The low-intensity XRD peaks indicate that the films consist of coarsely fine grains and/or are nanocrystalline in nature. The broad hump is due to the amorphous glass substrate. Comparison of observed  $d$  values with standard  $d$  values confirms the sphalerite cubic (zinc blende type) nanocrystalline structures. The lattice parameter of films were calculated by using the relation

$$d = a / (h^2 + k^2 + l^2)^{1/2} \quad (1)$$

these values and  $III_0$  values have given been in Table 3 for CdS,  $\text{In}_2\text{S}_3$  and  $\text{In}_{1-x}\text{Cd}_x\text{S}$  thin films. As seen in Table 3, observed  $d$  values are not similar standard  $d$  values. Since CdS,  $\text{In}_2\text{S}_3$  and  $\text{In}_{1-x}\text{Cd}_x\text{S}$  thin films have some defect; observed  $d$  values are different from standard  $d$  values.

The crystallite size of thin films was calculated by using Scherrer's Formula

$$D = K\lambda / \beta \cos\theta \quad (2)$$

where  $D$  is crystallite size,  $\lambda$  is the X-ray wavelength used  $\beta$  is the angular line width of half maximum intensity,  $\theta$  is Bragg's diffraction angle and  $K$  is some constant. The average crystallite size was calculated by resolving the highest intensity peak. The grain sizes of  $\text{In}_2\text{S}_3$  and  $\text{In}_{1-x}\text{Cd}_x\text{S}$  thin films have been given in Table 4. As shown in Table 4, the grain sizes of  $\text{In}_{1-x}\text{Cd}_x\text{S}$  thin films are smaller than  $\text{In}_2\text{S}_3$  and CdS thin films.  $\text{In}_{1-x}\text{Cd}_x\text{S}$  thin films have different phases from CdS and  $\text{In}_2\text{S}_3$ .

### 3.2 Morphological studies

Scanning electron micrographs of  $\text{In}_{1-x}\text{Cd}_x\text{S}$ ,  $\text{In}_2\text{S}_3$  and CdS thin films are shown in Fig. 2. It can be noticed that the microstructure of  $\text{In}_{1-x}\text{Cd}_x\text{S}$  changes with the increasing of cadmium molar fraction. The main feature of these micrographs is the observation of two types of microstructures: (i) It is observed that the surfaces of the films were about uniform and covered glass substrate well without any voids, pinholes or cracks. (ii) Big white grains originating

**Table 3** X-ray data of the  $\text{In}_{1-x}\text{Cd}_x$ ,  $\text{In}_2\text{S}_3$  and  $\text{CdS}$  thin films

Sample	$2\theta$	$(d \text{ \AA})$	$(d \text{ \AA})$	$hkl$	$III_0$	$III_0$
	Observed	Standard	Observed		Standard	Observed
$\text{In}_2\text{S}_3$	21.30	4.1680	4.2680	211	25	68
	22.30	4.0368	3.9833	116	55	70
	30.30	2.9510	2.9474	222	100	100
	41.50	2.2018	2.1741	306	38	24
	45.40	1.9750	1.9960	309	65	29
	50.60	1.8220	1.8024	413	35	37
$\text{CdS}$	26.50	3.3599	3.3607	002	91	100
	28.30	3.1600	3.1509	101	100	71
	30.20	2.9000	2.9569	200	40	79
	36.20	2.4519	2.4794	102	29	48
	43.90	2.0580	2.0607	110	80	58
	52.10	1.7530	1.7540	112	38	60
$\text{In}_{0.2}\text{Cd}_{0.8}\text{S}$	21.10	4.1680	4.2070	211 ( $\text{In}_2\text{S}_3$ )	25	87
	26.70	3.3599	3.3360	002 ( $\text{CdS}$ )	91	100
	43.90	2.0580	2.0607	110 ( $\text{CdS}$ )	80	50
$\text{In}_{0.4}\text{Cd}_{0.6}\text{S}$	51.90	1.7530	1.7603	112 ( $\text{CdS}$ )	38	39
	21.10	4.1680	4.2070	211 ( $\text{In}_2\text{S}_3$ )	25	81
	26.70	3.3599	3.3360	002 ( $\text{CdS}$ )	91	100
	43.90	2.0580	2.0430	110 ( $\text{CdS}$ )	80	43
$\text{In}_{0.6}\text{Cd}_{0.4}\text{S}$	52.10	1.7530	1.7540	112 ( $\text{CdS}$ )	38	30
	22.20	4.1680	4.0010	211 ( $\text{In}_2\text{S}_3$ )	25	88
	26.80	3.3599	3.3238	002 ( $\text{CdS}$ )	91	100
$\text{In}_{0.8}\text{Cd}_{0.2}\text{S}$	44.40	2.0580	2.0386	309 ( $\text{In}_2\text{S}_3$ )	80	49
	22.20	4.1680	4.0010	211 ( $\text{In}_2\text{S}_3$ )	25	96
	26.60	3.3599	3.3483	002 ( $\text{CdS}$ )	91	98
	44.40	2.0580	2.0386	309 ( $\text{In}_2\text{S}_3$ )	80	51

**Table 4** The grain size of  $\text{In}_2\text{S}_3$ ,  $\text{CdS}$  and  $\text{In}_{1-x}\text{Cd}_x\text{S}$  thin films

$2\theta$	$hkl$	Grain Size (nm)					
		$\text{In}_2\text{S}_3$	$\text{CdS}$	$\text{In}_{0.2}\text{Cd}_{0.8}\text{S}$	$\text{In}_{0.4}\text{Cd}_{0.6}\text{S}$	$\text{In}_{0.6}\text{Cd}_{0.4}\text{S}$	$\text{In}_{0.8}\text{Cd}_{0.2}\text{S}$
21.10	211	34.40		23.52	25.40	22.51	22.93
26.70	002	–	69.16	24.20	27.30	21.18	20.78
43.90	110	–	36.45	28.30	28.12	–	–
51.90	112	–	37.63	26.54	25.51	–	–
44.40	413	36.64	–	–	–	18.2	19.92

probably from the from the  $\text{CdS}$  compound, since their number increases with the increasing of cadmium molar fraction.

**3.3 Optical absorption**

The energy band gaps of these films were calculated with the help of absorption spectra. To measure the energy band gap, we plotted  $(\alpha hw)^2$  versus  $(hw)$ . Where  $\alpha$  is the absorption coefficient and  $hw$  is the photon energy. The absorption coefficient  $\alpha$  is proportional to;

$$\alpha(hw) = B(hw - E_g)^n \tag{3}$$

where  $B$  is a constant and  $n$  is an index ( $n = 1, 2, 3, \dots$ ).

These graphs  $[(\alpha)^2 \text{ versus } (hw)]$  have been given in Fig. 3. The band gap energies of thin films have been then determined by the extrapolation of the linear regions on energy axis as shown in Fig. 3.

At 10 K, it is found that the band gap energies for  $\text{CdS}$ ,  $\text{In}_{0.8}\text{Cd}_{0.2}\text{S}$ ,  $\text{In}_{0.6}\text{Cd}_{0.4}\text{S}$ ,  $\text{In}_{0.4}\text{Cd}_{0.6}\text{S}$ ,  $\text{In}_{0.2}\text{Cd}_{0.8}\text{S}$  and  $\text{In}_2\text{S}_3$  thin films were 2.22 eV, 2.56 eV, 2.52 eV, 2.46 eV, 2.38 eV, 2.72 eV, respectively. The band gap energy value is decreasing with increasing Cadmium content. Band gap energy values for different temperature are given in Table 5. Band gap value of  $\text{In}_{1-x}\text{Cd}_x\text{S}$  thin film, that falls between

**Fig. 2** The SEM images of  $\text{In}_2\text{S}_3$ , CdS and  $\text{In}_{1-x}\text{Cd}_x\text{S}$  thin films

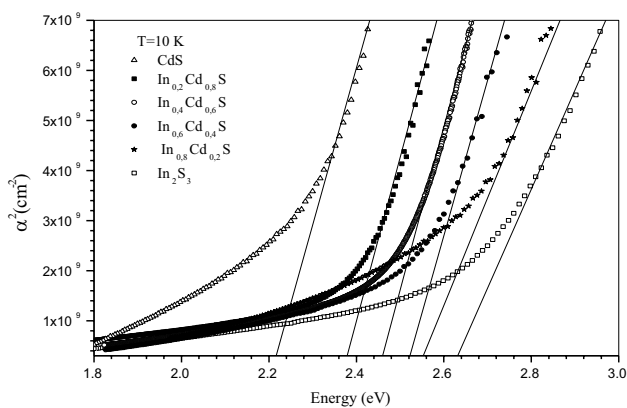
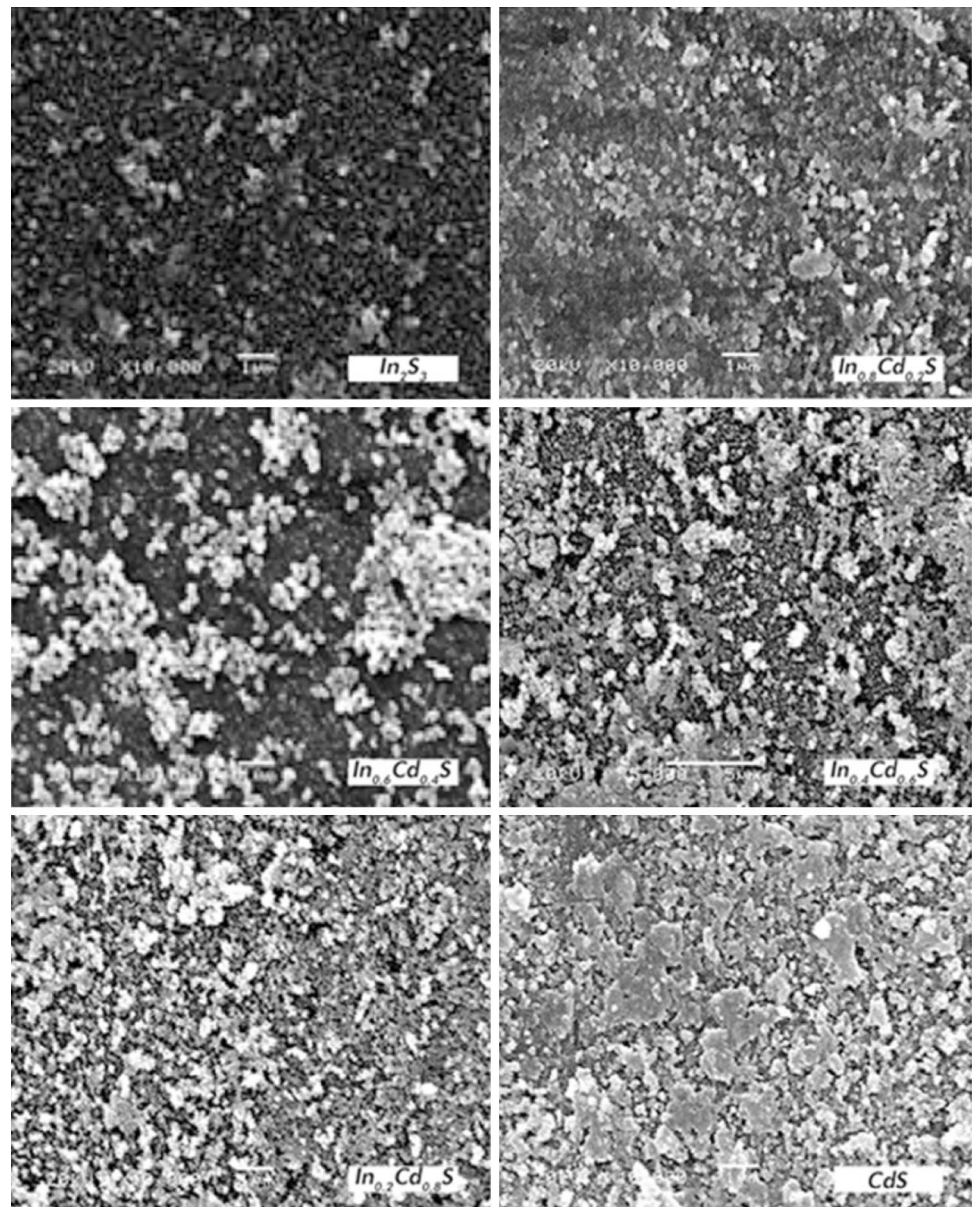


**Fig. 3**  $(\alpha)^2$  versus  $(h\nu)$  graph for CdS,  $\text{In}_2\text{S}_3$  and  $\text{In}_{1-x}\text{Cd}_x\text{S}$  thin films at 10 K

the band gap value of CdS and  $\text{In}_2\text{S}_3$  and these results are agreement with the literature [3, 5, 14, 15].

The refractive index of a material, along with the energy band gap, plays a fundamental role in the use of semiconductors and/or their mixed structures as electronic, optical and optoelectronic devices, as their properties are greatly influenced by the nature and magnitude of these two fundamental physical aspects. The fundamental correlation between these two factors employs the common concept of photoconductivity for semiconductors.

The refractive index of the films was calculated using Moss relation [22]:

$$E_g n^4 = k \quad (4)$$

**Table 5** The band gap energy values of In<sub>2</sub>S<sub>3</sub>, In<sub>1-x</sub>Cd<sub>x</sub>S and CdS thin films at 10, 100, 200 and 300 K

Sample	10 K	100 K	200 K	300 K
CdS	2.22	2.21	2.19	1.92
In <sub>0.2</sub> Cd <sub>0.8</sub> S	2.38	2.33	2.30	1.94
In <sub>0.4</sub> Cd <sub>0.6</sub> S	2.46	2.36	2.34	2.22
In <sub>0.6</sub> Cd <sub>0.4</sub> S	2.52	2.43	2.37	2.27
In <sub>0.8</sub> Cd <sub>0.2</sub> S	2.56	2.50	2.42	2.30
In <sub>2</sub> S <sub>3</sub>	2.72	2.68	2.62	2.45

where k is a constant with a value of 108 eV and E<sub>g</sub> is an energy band gap.

A different relation between the refractive index and band gap energy is presented by Herve and Vandamme [23, 24] in the following form:

$$n = \sqrt{1 + \left(\frac{A}{E_g + B}\right)^2} \tag{5}$$

where A and B are numerical constants with values of 13.6 and 3.4 eV, respectively.

The dielectric behavior of solids is important for several electron-device properties. Both static and high frequency dielectric constants were evaluated for all the films.

The high frequency dielectric constant (ε<sub>∞</sub>) was calculated from the following relation: [22]

$$E_\infty = n^2 \tag{6}$$

where n is refractive index.

The static dielectric constant (ε<sub>∞</sub>) of the films was calculated using a relation expressing the energy band gap dependence of ε<sub>∞</sub> for semiconductor compounds in the following form: [25]

$$\epsilon_0 = 18.52 - 3.08E_g \tag{7}$$

For 10 K, the calculated n, ε<sub>∞</sub> and ε<sub>0</sub> values of the In<sub>1-x</sub>Cd<sub>x</sub>S, In<sub>2</sub>S<sub>3</sub> and CdS thin films were presented in Table 6. As can be seen from the Table 6, for both Moss and Herve-Vandamme relations the refractive index value of In<sub>1-x</sub>Cd<sub>x</sub>S thin film falls between the refractive index value of CdS and In<sub>2</sub>S<sub>3</sub>. Noor et al. [26] have reported the first principles calculations of optical properties of Cd<sub>x</sub>Zn<sub>1-x</sub>S alloys. Laref et al. [27] have also simulated the optical properties of GaN, In<sub>x</sub>Ga<sub>1-x</sub>N, InN solar cell alloys. They demonstrated that the refractive indices rate follows the same trend as seen in Table 6. This result is consistent with the trend calculated here.

The refractive indices n as a function of temperature calculated using Eq. (4) for Moss relation and Eq. (5) for Herve-Vandamme relation is shown in Figs. 4 and 5,

**Table 6** The refractive indices (n), optical static dielectric constant (ε<sub>0</sub>), and optical frequency dielectric constant (ε<sub>∞</sub>) values of thin films at 10 K (MR: Moss Relation, HV: Herve\_Vandamme Relation)

10 K	ε <sub>0</sub>	n (MR)	ε <sub>∞</sub> (MR)	n (HV)	ε <sub>∞</sub> (HV)
CdS	11.68	2.641	6.97	2.618	6.85
In <sub>0.2</sub> Cd <sub>0.8</sub> S	11.18	2.595	6.73	2.557	6.53
In <sub>0.4</sub> Cd <sub>0.6</sub> S	10.94	2.574	6.62	2.527	6.38
In <sub>0.6</sub> Cd <sub>0.4</sub> S	10.75	2.558	6.54	2.506	6.27
In <sub>0.8</sub> Cd <sub>0.2</sub> S	10.63	2.549	6.49	2.491	6.20
In <sub>2</sub> S <sub>3</sub>	10.14	2.51	6.30	2.437	5.93

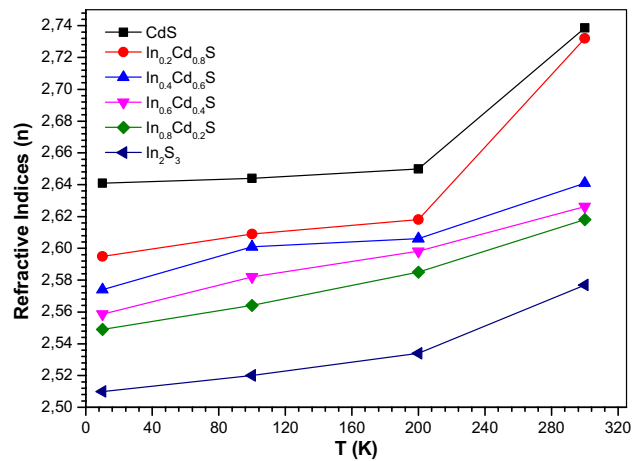


**Fig. 4** Refractive indices n calculated from Moss Relation as a function of temperature

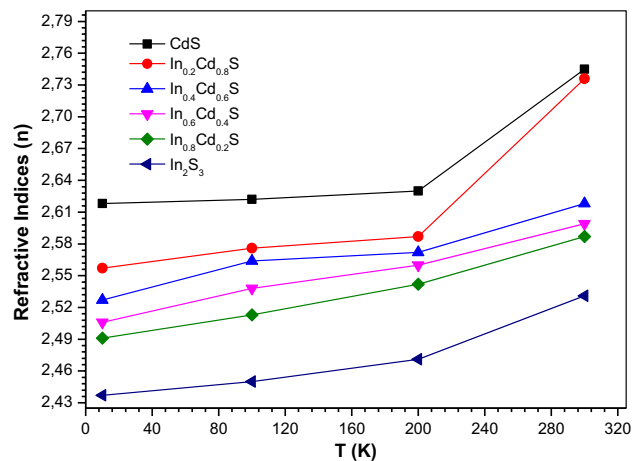


**Fig. 5** Refractive indices n calculated from Herve&Vandamme Relation as a function of temperature

respectively. As can be seen from the Fig. 4, the refractive indices values increased from 2.51 to 2.74 with increasing temperature. As can be seen from the Fig. 5,

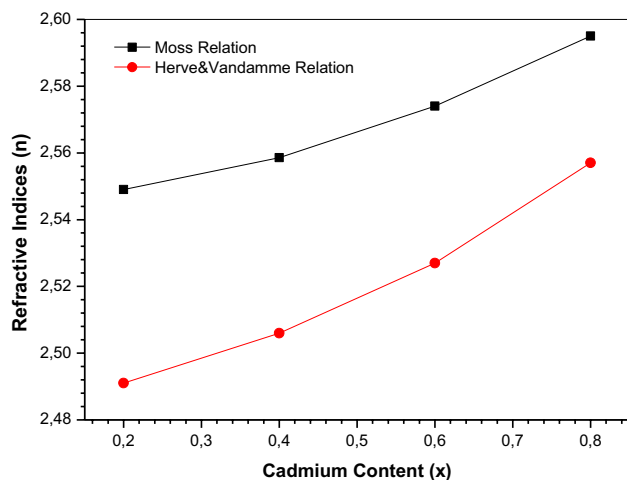


**Fig. 6** Refractive indices  $n$  as a function of Cadmium content  $\text{In}_{1-x}\text{Cd}_x\text{S}$  at 10 K

the refractive indices values increased from 2.43 to 2.74 with increasing temperature.

However the rate of increase seems to be dependent on the used models. Since  $n$  is strongly connected with band gap energy. Therefore, smaller band gap energy has a larger value of  $n$ .

Figure 6 shows the dependence of refractive indices on the Cadmium content for  $\text{In}_{1-x}\text{Cd}_x\text{S}$  ( $x=0.2, 0.4, 0.6, 0.8$ ) thin films. The refractive indices values are increasing with increasing Cadmium content. The refractive indices is dependent nonlinearly on the concentration.

### 3.4 Photoluminescence measurement

Measurement of PL emission at room temperature was made with Shimadzu RF-5301 PC spectrofluorimeter. The room-temperature PL emission spectrum of CdS,  $\text{In}_{1-x}\text{Cd}_x\text{S}$  and  $\text{In}_2\text{S}_3$  thin films is presented in Fig. 7 where the excitation wavelength was 500 nm. As shown in Fig. 7, the PL emission spectrums are very broadening and exhibit a high energy broad's band with maximums for CdS,  $\text{In}_{0.8}\text{Cd}_{0.2}\text{S}$ ,  $\text{In}_{0.6}\text{Cd}_{0.4}\text{S}$ ,  $\text{In}_{0.4}\text{Cd}_{0.6}\text{S}$ ,  $\text{In}_{0.2}\text{Cd}_{0.8}\text{S}$  and  $\text{In}_2\text{S}_3$  thin films were 2.221 eV, 2.308 eV, 2.289 eV, 2.261 eV, 2.222 eV, and 2.378 eV, respectively. Since CdS,  $\text{In}_2\text{S}_3$  and  $\text{In}_{1-x}\text{Cd}_x\text{S}$  thin films have some defect such as sulfur and indium vacancies, interstitial Cd atoms etc., the PL emission spectrums are very broad and differ from the absorption spectrum [1, 8]. The presences of defects are supported from XRD and electrical measurements.

### 3.5 Electrical properties

A thermoelectric (hot point probe) study was carried out for all prepared samples in order to identify the type of

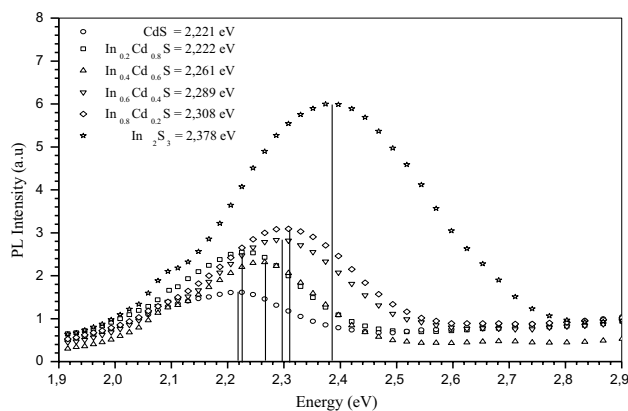


**Fig. 7** CdS,  $\text{In}_2\text{S}_3$  and  $\text{In}_{1-x}\text{Cd}_x\text{S}$  thin films photoluminescence spectra at room temperature

electrical conductivity of the deposited material. It was found that all of the films prepared in this work show n-type electrical conductivity. The electrical resistivity ( $\rho$ ) of the films deposited with different concentrations of Cd has been measured in the temperature range 300–450 K. Plots of  $\ln(\rho)$  vs.  $1/T$  for different Cd percentages are shown in Fig. 8. From the slopes of these plots, we have calculated the values of activation energies. The variation of room-temperature resistivity and activation energy ( $E_a$ ) with different concentrations of Cd is shown in Fig. 8. It is observed that the resistivity is decreasing with increasing temperature and this is confirming the semi conducting behavior and this variation is non-linear. Consisting of the film with discontinuous clusters and ionizing the impurity levels are two reasons of this non-linear behavior. The electrical resistivity is decreasing with in increasing temperature. The electrical resistivity values which were calculated at 300 K have been given in Table 7. Because  $\text{In}_{1-x}\text{Cd}_x\text{S}$  thin films have different phases from CdS and  $\text{In}_2\text{S}_3$ , the electrical resistivity values of these films are higher than CdS and  $\text{In}_2\text{S}_3$  thin films. The foreseen reasons for high resistivity are; nanocrystalline nature, crystallite boundary discontinuities, presence of defect states. As shown in Fig. 8, the activation energies were calculated for low and high temperature linear regions.

## 4 Conclusions

$\text{In}_{1-x}\text{Cd}_x\text{S}$ , CdS and  $\text{In}_2\text{S}_3$  thin films were grown by SILAR method a glass substrate at room temperature. These films are characterized by XRD and SEM.  $\text{In}_{1-x}\text{Cd}_x\text{S}$  thin films composed of cubic and hexagonal phases of  $\text{In}_2\text{S}_3$  and CdS. Optical band gap of  $\text{In}_{1-x}\text{Cd}_x\text{S}$  thin film was found to be in between band gaps of  $\text{In}_2\text{S}_3$  and CdS. The optical absorption studies show that these thin films have direct band gap



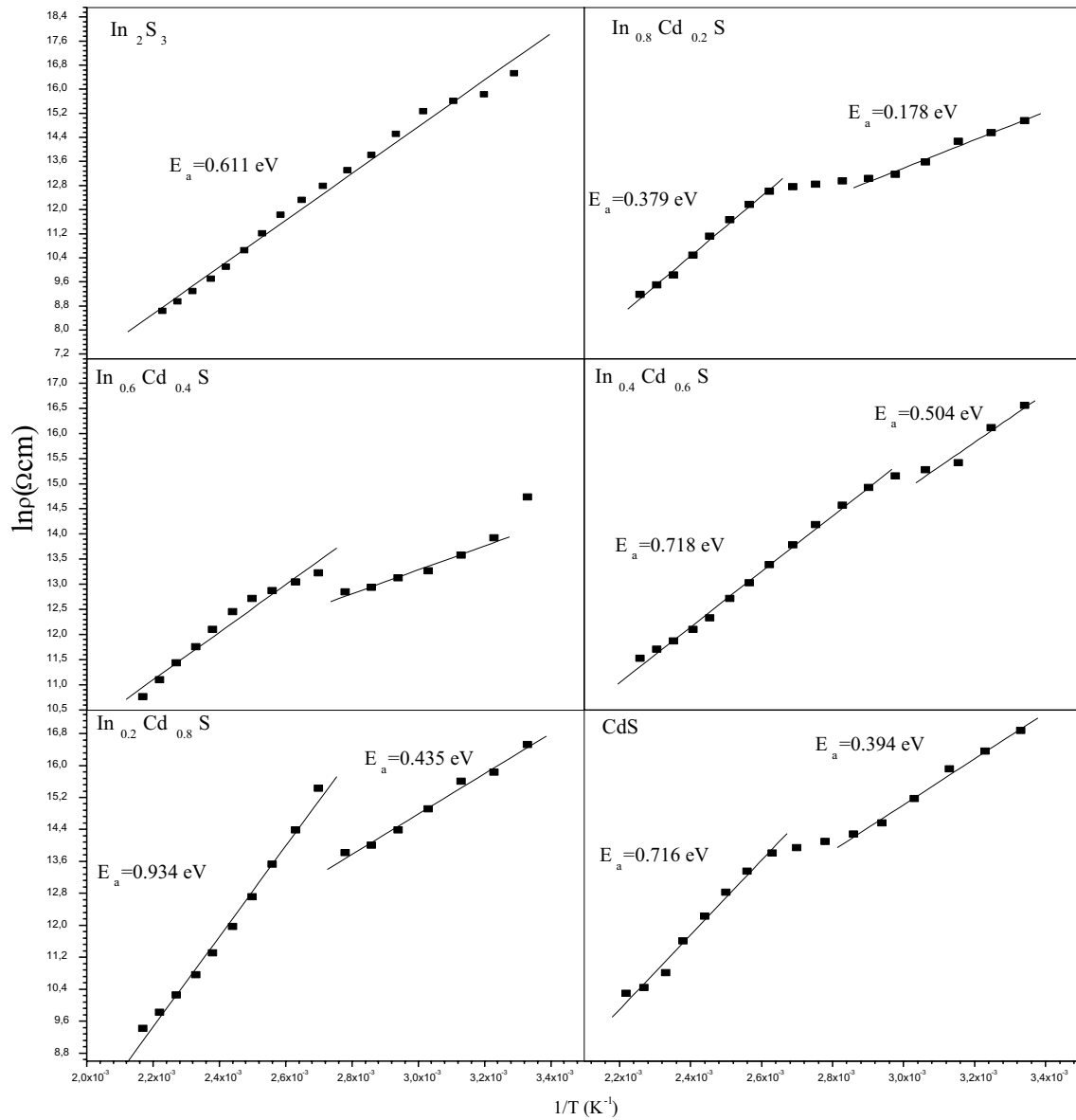


**Fig. 8** Variation of  $\log \rho$  versus  $1/T$  ( $K^{-1}$ ) for CdS,  $In_2S_3$  and  $In_{1-x}Cd_xS$  thin films

**Table 7** The resistivity of  $In_2S_3$ ,  $In_{1-x}Cd_xS$  and CdS thin films at 300 K

Sample	Resistivity ( $\Omega\text{cm}$ )
CdS	$1.4 \times 10^6$
$In_{0.2}Cd_{0.8}S$	$2.1 \times 10^7$
$In_{0.4}Cd_{0.6}S$	$4.3 \times 10^7$
$In_{0.6}Cd_{0.4}S$	$5.4 \times 10^7$
$In_{0.8}Cd_{0.2}S$	$6.2 \times 10^7$
$In_2S_3$	$7.5 \times 10^6$

and band gap energies for CdS,  $In_{0.8}Cd_{0.2}S$ ,  $In_{0.6}Cd_{0.4}S$ ,  $In_{0.4}Cd_{0.6}S$ ,  $In_{0.2}Cd_{0.8}S$  and  $In_2S_3$  thin films were found by 2.22 eV, 2.56 eV, 2.52 eV, 2.46 eV, 2.38 eV, 2.72 eV, respectively. As seen in Fig. 7, the PL measurement results

are compatible with absorbance measurements. The energy values are increasing with increasing Indium content. The PL emission spectrums are very broad because CdS,  $In_2S_3$  and  $In_{1-x}Cd_xS$  thin films have some defect such as sulfur and indium vacancies, interstitial Cd atoms etc.,. The presences of defects are supported from XRD and electrical measurements. The electrical resistivity of  $In_{1-x}Cd_xS$  thin films were about  $10^7 \Omega\text{-cm}$ . As a result, we can say that SILAR technique is suitable technique to deposit CdS,  $In_{1-x}Cd_xS$  and  $In_2S_3$  thin films.

The refractive indices values increased from 2.43 to 2.74 for all thin films with increasing temperature. However, the rate of increase seems to be dependent on the used models. Since  $n$  is strongly connected with band gap energy,

one may conclude that the smaller band gap energy material has a larger value of the  $n$ . The refractive indices values are increasing with increasing Cadmium content. Also, we studied static and high frequency dielectric constants ( $\epsilon_0, \epsilon_\infty$ ). As a result, we can say that SILAR technique is suitable technique to deposit CdS,  $\text{In}_{1-x}\text{Cd}_x\text{S}$  and  $\text{In}_2\text{S}_3$  thin films.

**Funding** This study was supported by Ataturk University Funding Project 2013300

## References

1. J. Aguilar-Hernandez, J. Sastre-Hernandez, R. Mendoza-Perez, G. Contreras-Puente, M. Cardenas-Garcia, J. Ortiz-Lopez, *Solar Energy Materials & Solar Cells* **90**, 704 (2006)
2. E. Çetinörgü, C. Gümüş, R. Esen, *Thin Solid Films* **515**, 1688 (2006)
3. S. Prabakar, M. Dhanam, *J. Cryst. Growth* **285**, 41 (2005)
4. X.L. Tong, D.S. Jiang, Y. Li, Z.M. Liu, M.Z. Luo, *Physica B* **382**, 105 (2006)
5. M. Kundakçı, A. Ateş, A. Astam and M. Yıldırım, *Physica E* **40/3**, 600 (2008)
6. A. Ateş, M. A. Yıldırım, M. Kundakçı and M. Yıldırım, *Chinese Journal of Physics* **45/2-I**, 182 (2007)
7. Teny Theresa John, Meril Mathew, C. Kartha Sudha, K. P. Vijayakumar, T. Abe, Y. Kashiwaba, *Solar Energy Materials & Solar Cells* **89**, 27 (2005)
8. R. Jayakrishnan, Teny Theresa John, C. Sudha Kartha, K. P. Vijayakumar, T. Abe and Y. Kashiwaba, *Semicond. Science and Technol.* **20**, 1162 (2005)
9. R.K. Sharma, S.T. Lakshmikummar, Singh Gurmeet, A.C. Rastogi, *Mater. Chem. Phys.* **92**, 240 (2005)
10. M. Calixto Rodriguez, A. Tiburcio Silver, A. A. Ortiz, Sanchez-Juarez, *Thin Solid Films* **480–481**, 133 (2005)
11. N.M. El-Nahass, B.A. Khalifa, H.M. Soliman, M.A.M. Seyam, *Thin Solid Films* **515**, 1796 (2006)
12. A. Timoumi, H. Bouzouita, M. Kanzari, B. Rezig, *Thin Solid Films* **480–481**, 124 (2005)
13. B. Asenjo, A.M. Chaparro, M.T. Gutierrez, J. Herrero, C. Maffiotte, *Thin Solid Films* **480–481**, 151 (2005)
14. M.G. Sandoval Paz, M. Sotelo-Lerma, J.J. Valenzuela Jauregui, R. M. Flores-Acosta, Ramirez Bon. *Thin Solid Films* **472**, 5 (2005)
15. H.M. Pahtan, C.D. Lokhande, S. S. Kulkarni. *Materials Research Bulletin* **40**, 1018 (2005)
16. R. Ranjith., T. John, C. Kartha., K.P. Vijayakumar., T. Abe., Y. Kashiwaba. *Materials Science in Semiconductor Processing*, **10**, 49 (2007)
17. M. Kundakçı, Y. Akaltun, A. Astam, A. Ateş, M. Yildirim, and B. Gürbulak, *AIP Conference Proceedings*, **899**, 1 (2007)
18. N.M. Ravindra, Preethi Ganapathy, Jinsoo Choi, *Infrared Physics & Technology* **50**, 21 (2007)
19. Y.F. Nicolau., *Appl. Surf. Sci.*, **22/23**, 1061 (1985)
20. T.D. Dzhafarov, F. Ongul, I. Karabay, *J. Phys. D: Appl. Phys* **39**, 3221 (2006)
21. X. Chen, Z. Zhang, X. Zhang, Liu, Y, Qian. *Chem. Phys. Lett.* **407**, 482 (2005)
22. L. Hannachi, N. Bouarissa, *Physica B* **404**, 3650 (2009)
23. F. Mezrag, W.K. Mohamed, N. Bouarissa, *Physica B* **405**, 2272 (2010)
24. P. Herve, L.K.J. Vandamme, *Infrared Phys. Technol* **35**, 609 (1994)
25. S. Adachi Wiley, Chishester (2005)
26. N.A. Noor, N. Ikram, S. Ali, S. Nazir, S.M. Alay-e-Abbas, A. Shaukat, *J. Alloys Compd.* **507**, 356 (2010)
27. A. Laref, A. Altujar, S.J. Luo, *The European Physical Journal B* **86**, 475 (2013)